J. Shanghai Jiao Tong Univ. (Sci.), 2017, 22(5): 570-576
https://doi.org/10.1007/s12204-017-1876-7

Fatigue Sensitivity Analysis of Steel Catenary Riser near Touchdown Point

WANG Kunpeng[1*] (王坤鹏), *JI Chunyan*[1] (嵇春艳), *XUE Hongxiang*[2] (薛鸿祥), *TANG Wenyong*[2] (唐文勇)
(1. School of Naval Architecture and Ocean Engineering, Jiangsu University of Science and Technology, Zhenjiang 212003, Jiangsu, China; 2. State Key Laboratory of Ocean Engineering, Shanghai Jiao Tong University, Shanghai 200240, China)

Abstract: By transforming the platform response obtained from coupled hydrodynamic analysis to the top motions of steel catenary riser (SCR), the nonlinear dynamic analysis of the SCR is carried out in Abaqus/Aqua. In this analysis, the SCR-seabed interaction is well taken into account by introducing the seabed trench model and hysteretic seabed model. The fatigue damage of the SCR near touchdown point (TDP) is calculated using rain-flow counting methodology, and the sensitivity of the fatigue damage to the seabed and wave parameters are investigated. The results indicate that as seabed stiffness increases, the fatigue life and its sensitivity to seabed stiffness decrease. Seabed trenching may benefit the fatigue life of the SCR and the trench position should be elaborated for realistic fatigue damage prediction. Due to the induced platform response, significant wave height and spectral peak period have significant effects on the fatigue damage, thus the short-term sea state bins should be carefully selected from the wave scatter diagram.
Key words: touchdown point, fatigue sensitivity, seabed trench, hysteretic seabed model
CLC number: P 752 **Document code:** A

0 Introduction

During the last decades, the experience of deepwater steel catenary risers (SCRs) application for oil and gas production shows that SCRs are economic and reliable riser systems, and have been adopted for many deepwater projects developed with floating hosts. However the complex environment loads applied to SCRs make the design very difficult. At the touchdown zone, the seabed reaction force is very difficult to determine, and the discrepancy of predicted fatigue life due to the difference of seabed stiffness and trench model is very distinct[1]. In addition to the riser-soil interaction, a large proportion of total fatigue damage results from riser top motions, so wave induced vessel motions would contributes significantly to the fatigue performance[2]. Xu et al.[3] studied the fatigue life of SCRs with semi-submersible and spar platforms, and the result showed that SCR with spar is more durable. Power et al.[4] neglected the seabed action and gave a comparative analysis between spectral method and rain-flow counting method on fatigue life. Fu and Yang[5] analyzed the effect of environment loads on SCR's fatigue life, in which the seabed was simplified as nonlinear spring and the coupled effect of platform system was not considered. Bai et al.[6] implemented a nonlinear *p-y* model into finite element code for riser analysis, Cable3D, and investigates the response and fatigue damage of a SCR at touchdown point (TDP). Elosta et al.[7] studied the seabed trenching on the fatigue life at touchdown zone. However, the obtained trench is very shallow, thus this cannot reflect the effect of seabed trench in the service life of the SCR. Fatigue life is one of the most important factors considered in the design of risers, so the assessment of the SCR's fatigue life using a scientific and feasible method is very important for the safety and economy of the offshore industry.

This study takes the platform, SCR and mooring lines as a whole, and carries out coupled analysis using commercial software, DeepC. By transforming the platform response to the SCR top motions, the global analysis of the SCR is then conducted in nonlinear finite element software, Abaqus/Aqua. In order to well simulate the SCR-seabed interaction, the seabed trench induced by SCR contact and hysteretic seabed resistance are taken into account by creating touchdown element based on user-define element (UEL) in Abaqus. Based

Received date: 2016-04-02
Foundation item: the Natural Science Foundation of Jiangsu Province (No. BK20160557), the National Natural Science Foundation of China (Nos. 51579146, 51490674), Shanghai Rising-Star Program (No. 16QA1402300)
∗**E-mail:** wangkunpeng@just.edu.cn

on the obtained stress history, the fatigue damage of the SCR near TDP is calculated using the curve of stress range versus number of stress cycles to fatigue failure (S-N curve) and rain-flow counting methodology. Next, the sensitivity of fatigue damage to seabed and wave parameters is investigated, and some conclusions are obtained.

1 Semi-Submersible System Parameters

The targeted SCR serves in a semi-submersible platform system for oil production. The platform has the dimension of 114 m × 78 m, mainly consists of four columns and two pontoons. The operational/survival draft is 19 m, and the related displacement is about 51 700 t. In this study, the operational water depth is 1.219 2 km.

Figure 1 illustrates that the platform is equipped with a 12-point spread mooring system. The mooring length is 3.950 km, with the form of chain-wire-chain. The key parameters of the targeted SCR are presented in Table 1, where D and t are the SCR diameter and thickness, respectively, C_{M} and C_{D} are the inertia coefficient and drag coefficient, respectively.

Table 1 Principals of the targeted SCR

Length/km	Departure angle/(°)	Wet weight/(kg · m^{-1})	Dry weight/(kg · m^{-1})	D/m	t/m	C_{M}	C_{D}
2.050	14	148.2	276.9	0.4	0.02	2.0	1.0

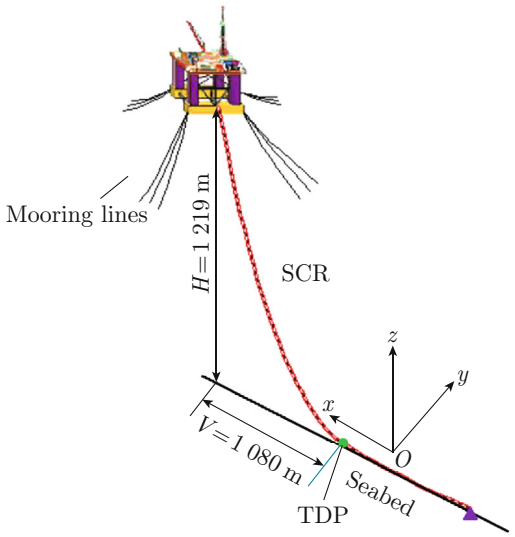

Fig. 1 Sketch of coupled semi-submersible platform system

2 Environment Loads

2.1 Wave and Current Load

The platform, SCR and mooring lines are coupled as a whole system. The coupled analysis software, DeepC for moored floating structure is therefore utilized to simulate the response of the platform system. Before this analysis, the wave frequency-dependent coefficients, such as added mass, radiation damping and wave-excitation force, are calculated based on the diffraction/radiation program, HydroD. In DeepC, the wave-excitation force is converted to the force in time domain, and the frequency-dependent radiation damping is included in form of convolution integral. As for the current force exerted on the platform, only the quadratic term is considered in this study, and can be expressed as follows:

$$F_{\mathrm{c}} = C_{\mathrm{Q}}(\beta)\,|\boldsymbol{u}(t)|^2\,, \tag{1}$$

$$|\boldsymbol{u}|^2 = (u_1 - \dot{x}_1)^2 + (u_2 - \dot{x}_2)^2, \tag{2}$$

$$\beta = \arctan\left(\frac{u_2 - \dot{x}_2}{u_1 - \dot{x}_1}\right), \tag{3}$$

where C_{Q} is quadratic current force coefficient; $\boldsymbol{u}$ is the relative velocity between current and platform; u_1 and u_2 are current velocity components along x- and y-axis; $\dot{x}_1$ and $\dot{x}_2$ are platform velocity in surge (x-axis) and sway (y-axis) directions respectively; β is relative current angle. C_{Q} is related to the projected area and shape of the platform, and can be calculated according to American Petroleum Institute (API)[8].

SCR and mooring lines belong to long slender structures, thus Morrison theory can be used for the description of wave and current loads. The Morrison force per unit length could be expressed as:

$$\boldsymbol{f} = \frac{1}{2}\rho C_{\mathrm{D}} D\,|\boldsymbol{U} - \boldsymbol{U}_{\mathrm{b}}|\,(\boldsymbol{U} - \boldsymbol{U}_{\mathrm{b}}) + \rho C_{\mathrm{m}} A(\dot{\boldsymbol{U}} - \dot{\boldsymbol{U}}_{\mathrm{b}}) + \rho A\dot{\boldsymbol{U}}, \tag{4}$$

where $\boldsymbol{U}$ and $\dot{\boldsymbol{U}}$ represent the fluid velocity and acceleration respectively; $\boldsymbol{U}_{\mathrm{b}}$ and $\dot{\boldsymbol{U}}_{\mathrm{b}}$ represent the velocity and acceleration of the slender structures; ρ is ambient fluid density; $C_{\mathrm{M}} = C_{\mathrm{m}} + 1$, C_{m} is added mass coefficient; A represents the riser cross-sectional area.

The wave scatter diagram in South China Sea is selected to simulate the sea environment, and is condensed to 6 bins presented in Table 2. The short-term sea state is depicted using the Joint North Sea Wave Project (JONSWAP) spectrum, and is assumed to have equal probability for different wave directions. The direction is 0° representing the wave propagates along

positive x-axis, and 90° representing the wave propagates along positive y-axis. The current is aligned with wave, and remains constant in the sea surface for all sea states. An approximate current profile based on the literature[9-10] is applied, and is presented in Table 3.

Table 2 Short term sea state for fatigue analysis

Sea state	Significant wave height/m	Wave peak period/s	Surface current velocity/ $(\mathrm{m}\cdot\mathrm{s}^{-1})$	Occurrence probability/%
S_1	1.25	5.3	0.9	53.40
S_2	1.75	5.3	0.9	18.00
S_3	2.25	5.3	0.9	11.70
S_4	2.75	5.3	0.9	7.74
S_5	3.75	7.5	0.9	5.16
S_6	4.25	7.5	0.9	4.01

Table 3 Current profile data

Distance to seabed/km	Current velocity/$(\mathrm{m}\cdot\mathrm{s}^{-1})$
1.219 2	0.90
1.050	0.52
0.880	0.30
0.500	0.15
0	0.03

The nonlinear finite element software, Abaqus/Aqua, is employed to carry out detailed global analysis of the SCR. The floating system responses are firstly calculated using DeepC, in which the hull drag and the hydrodynamic load of SCR and mooring lines are taken into account based on Eqs. (1)—(3) and Eq. (4), respectively. Then the platform responses are transformed as the SCR top motions in Abaqus to guarantee reasonable prediction of the SCR response. It is noted that since this study focuses on the fatigue damage near TDP, the flex joint connecting SCR and platform is not considered in the simulation.

2.2 Seabed Model

SCR-seabed interaction is the key aspect and challenging issue in the fatigue design of SCRs. Due to repeated contact between SCR and seabed, seabed trench would develop gradually, and in turn affects the SCR response at touchdown zone[11]. Since the seabed trench becomes stationary after several months following the installation of SCRs, an initial trench profile can be applied in the SCR global analysis[12]. By comparing different trench profiles in literature, Wang and Low[12] found that a cubic polynomial model can well delineate the trench profile:

$$d(\hat{x}) = d_{\max}\left[c_1\left(\frac{\hat{x}}{L_{\mathrm{T}}}\right)^3 + c_2\left(\frac{\hat{x}}{L_{\mathrm{T}}}\right)^2 + c_3\left(\frac{\hat{x}}{L_{\mathrm{T}}}\right)\right], \quad (5)$$

$$\left.\begin{aligned} c_1 &= -\frac{2\lambda-1}{[\lambda(\lambda-1)]^2} \\ c_2 &= \frac{3\lambda^2-1}{[\lambda(\lambda-1)]^2} \\ c_3 &= -\frac{3\lambda^2-2\lambda}{[\lambda(\lambda-1)]^2} \\ \lambda &= \frac{L_{\max}}{L_{\mathrm{T}}} \end{aligned}\right\}, \quad (6)$$

where $d_{\max}$ represents the trench depth at trench maximum depth point (TMP), see Fig. 2; $\hat{x}$ is the distance to trench beginning point (TBP); $L_{\max}$ and L_{T} are the distance from TMP to TBP and the trench length respectively;. d_{SW} is self-weight penetration; TEP means trench end point. It should be noted that this trench profile (TP) neglects the self-weight penetration since it can be formed in the numerical simulation.

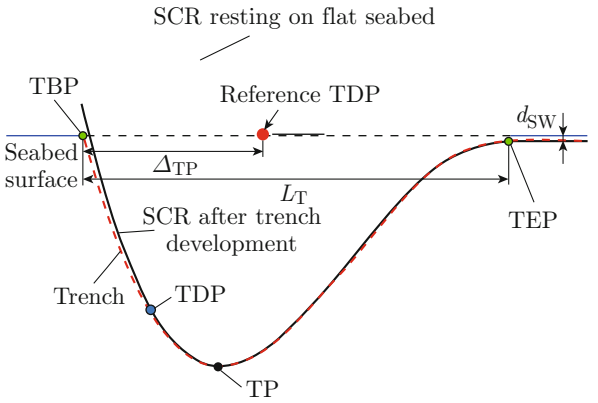

Fig. 2 Sketch of trench profile[12]

In order to match the trench profile with the touchdown zone, two parameters should be determined: L_{T} and Δ_{TP} (the distance from TBP to the reference TDP) shown in Fig. 2. Wang and Low[12] normalized the two parameters to R_{L} and R_{TP} respectively by divided by riser diameter, and obtained their relationship with normalized trench depth R_{d}, riser mass R_{M} and the ratio of horizontal and vertical span R_{HV} by solving an optimization problem. For saving space, this study would not detail this method, and just gives the corresponding equations:

$$\left.\begin{aligned} R_{\mathrm{L}} = {} & 72.5 + 30.9R_{\mathrm{d}} + 106.1R_{\mathrm{HV}} - \\ & 17.2R_{\mathrm{M}} - 3.38R_{\mathrm{d}}^2 + \\ & 46.2R_{\mathrm{d}}R_{\mathrm{HV}} \\ R_{\mathrm{TP}} = {} & -99.2 - 12.7R_{\mathrm{d}} + 48.8R_{\mathrm{M}} - \\ & 30R_{\mathrm{HV}} + 13.5R_{\mathrm{d}}^2 - 8.2R_{\mathrm{M}}^2 - \\ & 12.1R_{\mathrm{d}}R_{\mathrm{HV}} \end{aligned}\right\}, \quad (7)$$

$$\left.\begin{aligned} R_{\mathrm{d}} &= d_{\max}/D \\ R_{\mathrm{M}} &= 4m/(\rho\pi D^2) \\ R_{\mathrm{HV}} &= H/V \end{aligned}\right\} \tag{8}$$

where m represents the wet weight of the SCR per unit length; H and V represent the horizontal and vertical span of catenary zone respectively (see Fig. 1).

According to the large scale SCR test data, Bridge et al.[13] indicated that the seabed resistance and SCR penetration yields to hysteretic relationship. This study applies the linear hysteretic seabed model[14] to simulate the SCR-soil interaction, as shown in Fig. 3. The initial penetration curve can be described by the following equation, which governs the relationship between seabed resistance (P) and penetration (d) of Point 1.

$$\left.\begin{aligned} P &= N_{\mathrm{P}} D(S_0 + S_{\mathrm{g}} d) \\ N_{\mathrm{P}} &= a(d/D)^b \end{aligned}\right\}, \tag{9}$$

where S_0 and S_{g} represent mudline shear strength and shear strength gradient respectively; N_{p} is a dimensionless bearing factor; a and b are empirical parameters taken to be 6.7 and 0.254 respectively[15].

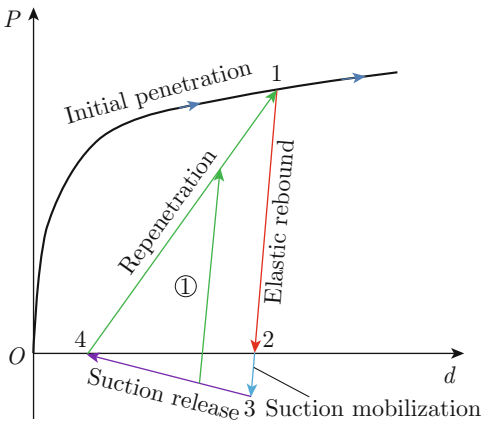

Fig. 3 Linear hysteretic SCR-seabed interaction model

Combined with the trench model, the penetration of Point 1 can be determined using Eq. (5). As shown in Fig. 3, when SCR uplifts, the seabed resistance would decrease to zero from Point 1 to Point 2, and then the soil suction mobilizes from Point 2 to Point 3, and releases from Point 3 to Point 4 until SCR separates with seabed. When the SCR turn to move downwards without SCR-seabed separation, the resistance would follow Line ① which is parallel to the elastic rebound curve.

Based on the trench model and linear hysteretic SCR-seabed interaction model, a touchdown element is developed by using the user subroutine UEL in Abaqus. This can guarantee reasonable response of SCR at touchdown zone in the global simulation. Figure 4 demonstrates the numerically obtained resistance-penetration relationship near TDP using the touchdown element under $S_0 = 2.5\,\mathrm{kN}$, $S_{\mathrm{g}} = 2.5\,\mathrm{kN/m}$, $d_{\max} = 1.0\,\mathrm{m}$. It can be seen that the mobilization and release of the soil suction is well captured as expected.

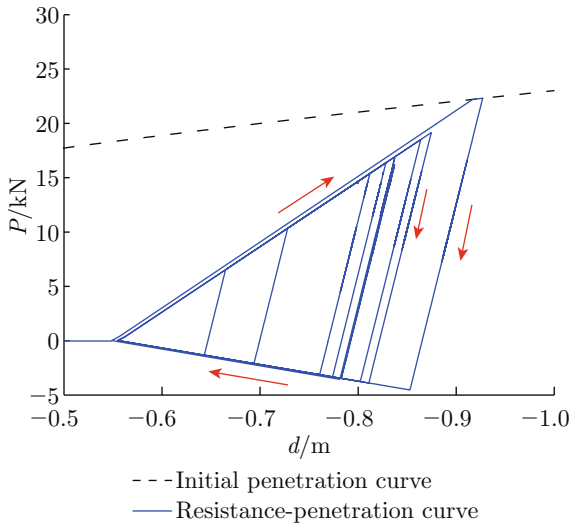

Fig. 4 Numerically obtained seabed resistance-penetration relationship

3 Fatigue Sensitivity Analysis

This study assumes that the material fatigue damage of SCR obeys Miner's rule[16], and the Notation D S-N curve considering the cathodic protection in seawater recommended by Det Norske Veritas (DNV)[17] can represent the material performance. The stress history is calculated by combining the stress induced by axial force and bending moment[18], based on that the stress cycles with different ranges are obtained by rain-flow counting methodology. In this study, the simulation time is 1 500 s for all cases.

3.1 Effect of Seabed Stiffness

For the study of the sensitivity of TDP's fatigue damage to the seabed stiffness, four S_0 with constant $S_{\mathrm{g}} = 2.5\,\mathrm{kN/m}$ are used: 1.5 kN, 2.5 kN, 3.5 kN and 4.5 kN. The seabed trench depth $d_{\max}$ is set to 2 times riser diameter (i.e. $R_{\mathrm{d}} = 2.0$). According to the SCR parameters, the seabed trench can be configured to match with the SCR at touchdown zone. The fatigue life as a function of S_0 is illustrated in Fig. 5. It can be seen that the predicted fatigue life decreases with the increasing S_0, and changes quickly in low stiffness zone, but slowly in high stiffness zone. This trend is in good agreement with that in Ref. [19].

Figure 6 gives the relationship between stress range and the number of stress cycles under S_6 with wave direction of 0°. Most of the stress range (τ) concentrates in 1—15 MPa, and the whole number of stress cycles almost remains constant under different seabed stiffness. If the stress range corresponding to Nos. 1—5 and No. 6 is considered as low and high range zone respectively, the bar chart shows that low seabed stiffness gives more

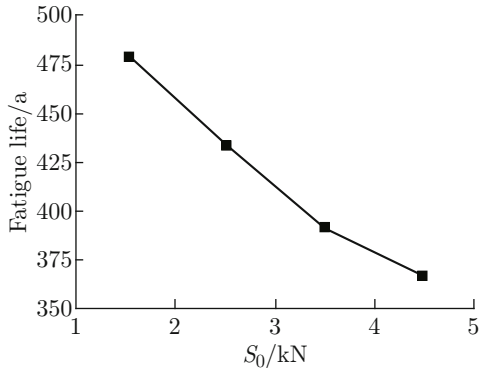

Fig. 5 Seabed stiffness effect on TDP's fatigue life

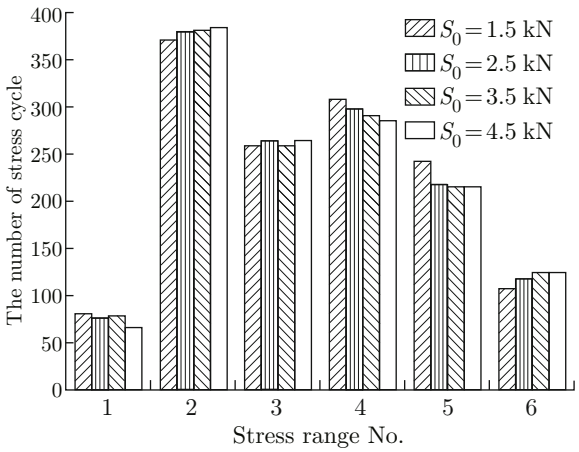

No. 1 — τ =0-1 MPa No. 2 — τ =1-2 MPa
No. 3 — τ =2-3 MPa No. 4 — τ =3-5 MPa
No. 5 — τ =5-15 MPa No. 6 — τ >15 MPa

Fig. 6 The cycle number of different stress ranges

low stress range cycles, but high seabed stiffness gives more high stress range cycles. From the above analysis, it can be concluded that the decrease of low stress range cycles and the increase of high stress range cycles are the main reason for lower fatigue life in stiffer seabed conditions.

3.2 Effect of Seabed Trench

Traditional approach usually applies flat seabed without considering the trench effect. This may result in conservative stress near TDP[20]. By setting different R_d, this study investigates the effect of trench development on the fatigue damage near TDP. Figure 7 indicates that the fatigue damage decreases with increasing R_d, so trench development may benefit the fatigue life of the SCR. The reason may be that with trench development the stress near TDP can be distributed along a larger length of SCR at touchdown zone, thus reduces the stress peak value.

Next, the effect of the trench position on the fatigue damage is studied, and the result is shown in Fig. 8. It is noted that the positive relative position means the seabed trench (base trench) obtained from Eq. (7) moving toward to bottom end. Figure 8 divides the relative position into three regions according to the matching between seabed trench and static SCR. Region 1 represents that SCR contacts TBP. Region 2 represents that TDP is located between TBP and TMP. Region 3 represents that SCR just lies on the trench between TMP and TEP. It can be seen that if the trench position is unreasonable, the fatigue damage may be overestimated or underestimated. At Region 3, the fatigue damage is slightly overestimated, but still lower than that corresponding to the flat seabed. For Region 1, due to the intensive contact at TBP, the fatigue damage is significantly overestimated. At the boundary between Region 1 and Region 2, the fatigue damage is underestimated. The reason is that the SCR slightly contacts the seabed at TBP, which alleviates the stress near TDP, so the fatigue damage is mitigated, and a little peak near TBP circled in Fig. 9 occurs.

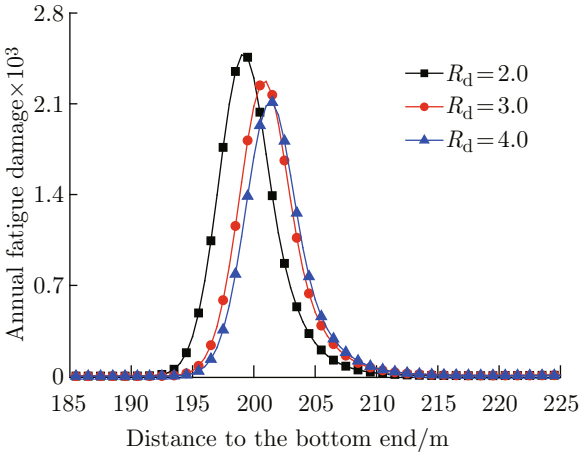

Fig. 7 Effect of trench depth on the annual fatigue damage

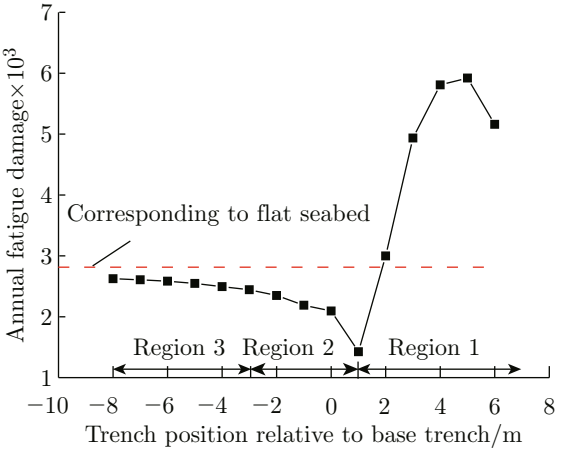

Fig. 8 Effect of the trench position on the annual fatigue damage

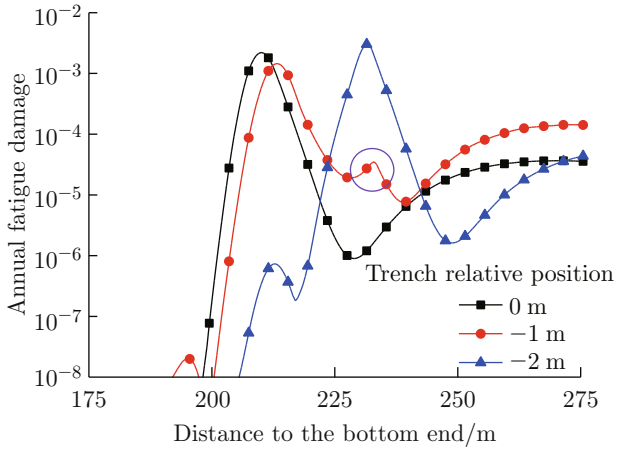

Fig. 9 Annual fatigue damage at touchdown zone

3.3 Effect of Wave Parameters

The SCR is connected with platform through a flexible joint, so the wave induced motions of platform have a significant effect on the TDP's response. This section would focus on the sensitivity of fatigue damage of the SCR near TDP to the wave parameters: H_S and T_P. The seabed model parameters are: $S_0 = 2.5\,\text{kN}$, $S_g = 2.5\,\text{kN/m}$, $R_d = 2$.

Figure 10 shows the annual fatigue damage of all states under different S_0. When T_P remains constant, TDP's fatigue damage almost has a linear relationship with H_S, and larger T_P corresponds to larger slope, so H_S and T_P both have a significant effect on TDP's fatigue damage, and the sensitivity of fatigue damage to H_S is related with T_P. It should be mentioned that the annual fatigue damage in Fig. 10 includes the occurrence probability of each state. Actually, in the wave scatter diagram, a sea state with larger H_S and T_P may not correspond to higher fatigue damage in the serve life of the SCR since this sea state may have very small occurrence probability. Therefore, it should be discreet when condensing the wave scatter diagram to fewer sea state bines for saving computational time.

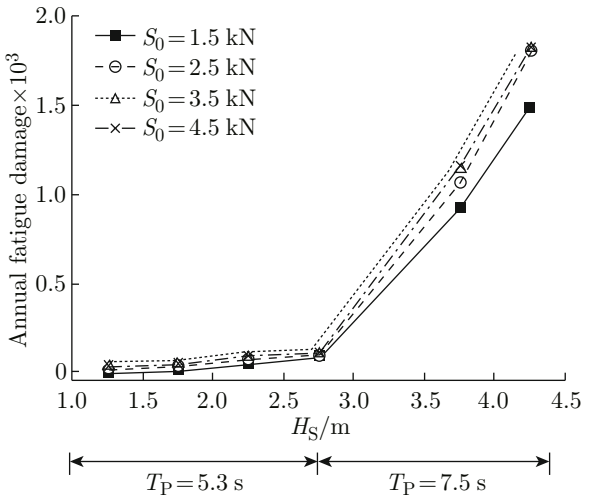

Fig. 10 Wave height and period effect on TDP's fatigue damage

4 Conclusion

In this paper the response of the selected semi-submersible platform system under different short-term sea states was predicted based on the coupled hydrodynamic analysis technology, and then transformed as the top boundary condition of the SCR for the global analysis in nonlinear finite element software, Abaqus. It should be mentioned that this study did not consider the second order wave force applied on the semi-submersible platform and the seabed lateral seabed stiffness, which will be investigated in the future work. In the global analysis of the SCR, the seabed model in literature is introduced for more realistic simulation of SCR-seabed interaction. The sensitivities of TDP's fatigue damage to seabed stiffness, seabed trench and wave parameters were then analyzed, and some reasonable conclusions were obtained.

Seabed stiffness has a great influence on the prediction of SCR's fatigue life near TDP. With seabed stiffness increasing, the stress cycles almost remain constant, but the cycle number of high stress range increases, thus the fatigue life decreases.

With trench development, the fatigue damage near TDP decreases. This indicates that the seabed trenching may benefit the fatigue life of SCR. If the trench position is not reasonably configured in the global analysis, the fatigue damage near TDP may be significantly overestimated or underestimated. Therefore, the trench position should be elaborated.

As spectral peak period T_P increases, the effect of the significant wave height H_S on TDP's fatigue damage becomes more significant. Therefore, the short-term sea states with low occurrence probability but large H_S and T_P should be deliberated when dividing the wave scatter diagram into condensed sea state bins.

References

[1] SHIRI H. Influence of seabed trench formation on fatigue performance of steel catenary risers in touchdown zone [J]. *Marine Structures*, 2014, **36**: 1-20.

[2] SONG R, STANTON P. Advances in deepwater steel catenary riser technology state-of-the-art: Part II. analysis [C]//*Proceedings of the ASME 2009 28th International Conference on Ocean, Offshore and Arctic Engineering*. Honolulu, Hawaii, USA: ASME, 2009: 79405.

[3] XU J, JESUDASEN A S, FANG J. Wave loading fatigue performance of steel catenary risers (SCRs) in ultradeepwater application [C]//*Offshore Technol-*

ogy Conference. Houston, Texas, USA: OTC Program Committee, 2006: 18180.

[4] POWER T L, MANIAR D R, GARRETT D L. Spectral and cycle-counting fatigue damage estimation methods for steel catenary risers [J]. *SPE Projects, Facilities & Construction*, 2008, **4**(4): 106-123.

[5] FU J J, YANG H Z. Fatigue characteristic analysis of deepwater steel catenary risers at touchdown point [J]. *China Ocean Engineering*, 2010, **24**(2): 291-304.

[6] BAI X L, HUANG W P, VAZ M A, et al. Riser-soil interaction model effects on the dynamic behavior of a steel catenary riser [J]. *Marine Structures*, 2015, **41**: 53-76.

[7] ELOSTA H, HUANG S, ATILLA I. Trenching effects on structural safety assessment of integrated riser/semisubmersible in cohesive soil [J]. *Engineering Structures*, 2014, **77**: 57-64.

[8] Recommended Practice 2SK. Design and analysis of station keeping system for floating structures [S]. Washington DC: American Petroleum Institute, 2005.

[9] Recommended Practice DNV-RP-C205. Environmental conditions and environmental loads [S]. Oslo: Det Norske Veritas, 2014.

[10] WILLIS N. Stride project-steel risers in deepwater environments — recent highlights [C]// *Proceedings of 24th Deepwater and Ultra Deepwater Riser Conference*. London: 2H Offshore Ltd, 2001: 2-12.

[11] NAKHAEE A, ZHANG J. Trenching effects on dynamic behavior of a steel catenary riser [J]. *Ocean Engineering*, 2010, **37**(2/3): 277-288.

[12] WANG K P, LOW Y M. A simple parametric formulation for the seabed trench profile beneath a steel catenary riser [J]. *Marine Structures*, 2016, **45**: 22-42.

[13] BRIDGE C, LAVER E, EVANS T. Steel catenary riser touchdown point vertical interaction models [C]//*Offshore Technology Conference*. Houston, USA: OTC Program Committee, 2004: 16628.

[14] WANG K P, XUE H X, TANG W Y. Dynamic response analysis of deepwater steel catenary riser based on the seabed-suction and stiffness-degradation model [J]. *Journal of Shanghai Jiao Tong University*, 2011, **45**(4): 585-586 (in Chinese).

[15] AUBENY C P, BISCONTON G. Seafloor-riser interaction model [J]. *International Journal of Geomechanics*, 2009, **9**(3): 133-141.

[16] MINER M A. Cumulative damage in fatigue [J]. *Journal of Applied Mechanics*, 1945, **12**(3): 159-164.

[17] Recommended Practice DNV-RP-C203. Fatigue design of offshore structures [S]. Oslo: Det Norske Veritas, 2005.

[18] Recommended Practice DNV-RP-F204. Riser Fatigue [S]. Oslo: Det Norske Veritas, 2005.

[19] RANDOLPH M, QUIGGIN P. Non-linear hysteretic seabed model for catenary pipeline contact [C]//*Proceedings of the ASME 2009 28th International Conference on Ocean, Offshore and Arctic Engineering*. Honolulu, USA: ASME, 2009: 79259.

[20] BRIDGE C, HOWELLS H A. Observations and modeling of steel catenary riser trenches [C]//*Proceedings of the 17th International Offshore and Polar Engineering Conference*. Lisbon, Portugal: ISOPE, 2007: 468.